

000 RANK-EFFICIENT MIXTURE OF EXPERTS FOR LLM 001 FINETUNING 002

003 **Anonymous authors**

004 Paper under double-blind review

005 ABSTRACT

006 Large language models (LLMs) have achieved impressive results in many general-
007 purpose domains, but their performance on specific tasks can still be improved
008 through finetuning. Parameter-efficient finetuning (PEFT) aims to tailor an LLM
009 to one or more tasks through a small amount of trainable parameters, requiring re-
010 duced computational resources. On the one hand, techniques like low-rank adap-
011 tation (LoRA) provide the required parameter efficiency with adapters of low, and
012 fixed, rank, which also limits their flexibility. On the other hand, Mixture of ex-
013 perts (MoEs) enhance the flexibility of a model at the cost of an increased param-
014 eter count and computational budget. The combination of the two approaches,
015 parameter-efficient MoEfication, has shown promise in addressing the issues of
016 both. In this work, we propose two methods that improve the rank-efficiency of
017 PEFT adapters, increasing the flexibility and reducing the number of parameters
018 involved in MoEfication. First, SharedLoRA retains the additive nature of LoRA
019 by using a two-tier structure of adapters, thereby **increasing the effective rank**
020 of the adapter while also reducing its size. Second, OperA **replaces additive**
021 with **quantum-inspired multiplicative interactions** to further drive rank effi-
022 ciency upwards and number of parameters downwards. We show that both tech-
023 niques match or surpass the state-of-the-art (SoTA) in its commonly used setup on
024 6 open-source frontier LLMs and 7 tasks, while using notably fewer parameters.
025 Moreover, we also find that **OperA is optimal given the same parameter budget**
026 for 5 out of 6 models considered, always using fewer parameters than the baseline.
027 Finally, we provide evidence for the superior performance of our methods by an-
028 alyzing the effective rank of the adapters. Here, our SharedLoRA nearly doubles
029 the rank of the SoTA solution, while our OperA’s rank is more than two orders of
030 magnitude greater.

031 1 INTRODUCTION

032 Large language models (LLMs) have demonstrated impressive capabilities (OpenAI, 2025; 2024;
033 Qwen AI, 2025a; Meta AI, 2024) when generalizing to novel tasks, making them the models of
034 choice for a variety of domains (Wang et al., 2024; Liu et al., 2024a; 2023). This success is in part
035 due to the vast datasets with which LLMs are pretrained, granting them general knowledge that is
036 then applied to each specific task. Nonetheless, it has been shown that LLMs can be further special-
037 ized (or finetuned) to improve performance in under-represented, and often especially challenging,
038 scenarios (Hu et al., 2022; Parthasarathy et al., 2024). This finetuning process is performed closer to
039 the end application, where data and computational resources are more scarce than in the pretraining
040 phase.

041 Nonetheless, full finetuning of an LLM still requires massive resources (Xia et al., 2024b) and is
042 unfeasible in many use-cases. Parameter-efficient finetuning (PEFT) has emerged as an effective
043 solution that dramatically reduces the computational costs associated with finetuning LLMs (Han
044 et al., 2024; Hu et al., 2022; Liu et al., 2024b). One of the most successful PEFT paradigms,
045 low-rank adaptation (LoRA; Hu et al. 2022), leverages low-rank approximations to adapt specific
046 subspaces of the full weight matrices, often recovering or even surpassing the performance of its
047 full-rank counterparts. The effectiveness of LoRA is likely a testament to the low-ranked nature of
048 task-specific subspaces in neural networks at large. This hypothesis is corroborated by the relatively
049 poorer performance of LoRA when applied to multiple tasks (Feng et al., 2024; Xia et al., 2024a),

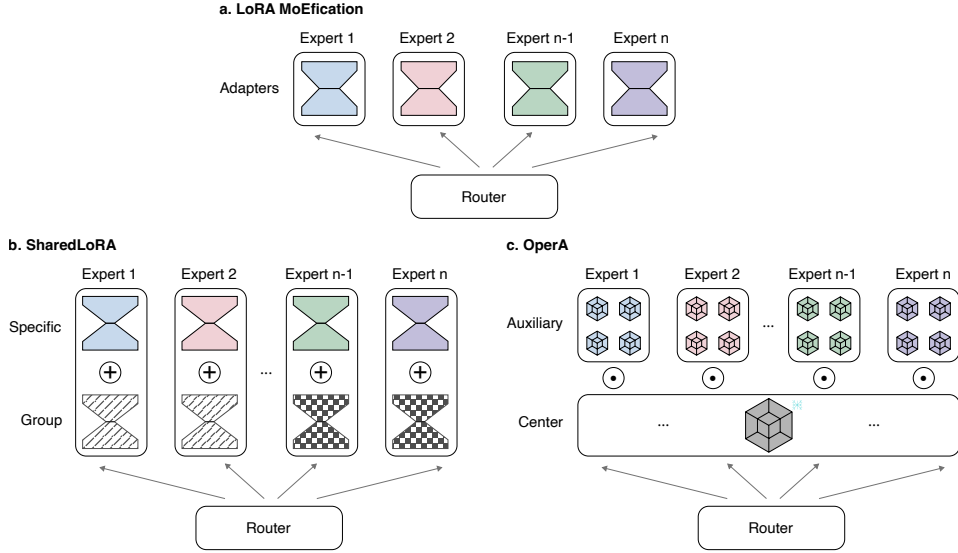


Figure 1: **Rank-efficient Mixture of experts.** **a.** Regular LoRA MoEification uses one low-rank adapter per expert. **b.** The experts of SharedLoRA are built by additively combining shared basis LoRAs with expert-specific LoRAs of the same rank. The SharedLoRA rank is therefore the sum of the two ranks. **b.** The experts of OperA are instead built through multiplicative combination of 4D cores, obtained by Matrix product operator (MPO) decomposition.

which can no longer be comfortably represented in low-rank subspaces, but instead require larger solutions.

At the same time, Mixture of experts (MoEs; Shazeer et al. 2017; Fedus et al. 2022) has been widely adopted in recent LLM architectures as a technique to improve performance across tasks without increasing the active parameter count (Jiang et al., 2024; IBM, 2024; DeepSeek-AI, 2025). MoEs leverage multiple linear models (aptly called experts) that process tokens in parallel, offering an attractive factorization of extremely large spaces into more manageable chunks. By instantiating a large number of experts, but only activating few of them for each token, LLMs can be internally specialized without significantly increasing computational costs. However, MoEs still suffer from increased memory requirements, as all experts need to be kept in memory even when not in use.

Finally, LoRAs and MoEs can be combined to obtain a PEFT approach that is parameter-efficient, memory-efficient, and is highly flexible (Tian et al., 2024; Li et al., 2024; Zeng et al., 2025). In particular, each expert is represented as a low-rank linear model, while maintaining the same gating and routing structure of regular MoEs (see Figure 1a), which have already been shown to be sufficiently powerful. Taken individually, each expert can only operate on a restricted subspace, and is therefore susceptible to the same weakness as LoRAs. However, the combination of multiple experts raises the flexibility of the overall model, thereby increasing performance.

We propose here two techniques that **both increase the effective rank (Roy & Vetterli, 2007) of the parameter-efficient MoE layer without increasing its parameter count**. Indeed, while the matrix rank might not be an adequate measure of the actual size of the subspace spanned by an adapter due to both practical and numerical reasons, the effective rank provides a more robust measure of the dimensionality of a matrix. First, we introduce SharedLoRA (see Figure 1b). SharedLoRA acts on the rank of the mixture itself, factorizing each expert into two tiers of adapters: (a) specific and (b) grouped. The specific adapters are entirely analogous to conventional low-rank adapters, with one adapter per desired expert. The grouped adapters instead form shareable bases that get added to the specific adapters to increase variety. The combination of specific and grouped adapters results in a reduction in the LoRA rank of each adapter, but in an increase in the rank of each expert.

The second technique we introduce does away with fixed-(and low-)rank adapters altogether by leveraging multiplicative interactions instead of additive ones. To do so, we borrow Matrix product operators (MPOs; Pirvu et al. 2010; Schollwöck 2011; Orús 2014) from the quantum physics liter-

108 ature to obtain OperA (see Figure 1c). MPOs provide an efficient multiplicative decomposition of
 109 arbitrary matrices (originally, Hamiltonians) into *core* and *auxiliary* 4D tensors. By choosing the
 110 MPO configuration carefully, we can concentrate most of the weights onto the core tensor and leave
 111 it fixed, while learning the leaner auxiliary tensors during training.

112 We evaluate SharedLoRA and OperA on a comprehensive set of 7 tasks, including ARC (Clark
 113 et al., 2018), PIQA (Bisk et al., 2020), OpenBookQA (Mihaylov et al., 2018), BoolQ (Clark et al.,
 114 2019), HellaSwag (Zellers et al., 2019), and WinoGrande (Sakaguchi et al., 2021), comparing them
 115 with MixLoRA (Li et al., 2024), the current openly available state-of-the-art (SoTA) technique for
 116 LoRA MoEfication. We test all approaches on multiple models of different sizes and from different
 117 sources to ensure the consistency of our evaluation, including Llama3, Llama3.1, Llama3.2 (Meta
 118 AI, 2024), Phi4 (Abdin et al., 2024), and Qwen2.5 (Qwen AI, 2025b). We find that our techniques
 119 achieve equal or superior results to SoTA techniques like MixLoRA (Li et al., 2024) and notably
 120 increase the effective rank as well, all while reducing the required number of parameters by 38%
 121 (SharedLoRA) and 62% (OperA) on average. Moreover, OperA achieves higher accuracy on 5 out
 122 of 6 models when given the same parameter budget.

123

124 2 RELATED WORKS

125

126 **Parameter-efficient finetuning (PEFT).** Modern open-weights frontier LLMs can reach tens of
 127 billions to hundreds of billions of parameters. Fully finetuning such models for downstream tasks
 128 can prove unfeasible in most situations, where parameter-efficient finetuning (PEFT) becomes a ne-
 129 cessity. The most popular approach to PEFT for LLMs is LoRA (Hu et al., 2022), which leverages
 130 low-rank matrices to finetune a low-dimensional subspace of the original weights to improve per-
 131 formance while reducing the required number of parameters. Further gains on parameter efficiency
 132 have been obtained by weight sharing (VeRA; Kopitzko et al. 2024), weight tying (Tied-LoRA; Ren-
 133 duchintala et al. 2024), quantization (QLoRA; Dettmers et al. 2023), and other techniques (Yang
 134 et al., 2025; Hayou et al., 2025). The downstream performance of LoRA has also been improved
 135 upon, especially through normalization (DoRA; Liu et al. 2024b).

136

137 **Mixture of experts (MoEs).** MoEs (Shazeer et al., 2017; Fedus et al., 2022) allow LLMs to ef-
 138 ficiently scale the number of parameters without proportionally scaling their compute budgets. In
 139 particular, MoEs are part of the conditional computing paradigm, where subsets of the full model are
 140 activated in an input-dependent manner. There are multiple variants of MoEs, especially depending
 141 on the routing (Fedus et al., 2022; Ruiz et al., 2021; Yue et al., 2025) and the gating mechanism (Li
 142 et al., 2023; Puigcerver et al., 2024). Recent works (DeepSeek-AI, 2025; Qwen AI, 2025a) have
 143 also shown that very large mixtures with few experts active at a time show remarkable performance
 144 across a wide variety of tasks.

145

146 **Parameter-efficient MoEfication.** The combination of PEFT with MoEs has recently started
 147 gaining traction (Dou et al., 2024; Tian et al., 2024; Li et al., 2024; Zeng et al., 2025), to address the
 148 limitations of both approaches. Most parameter-efficient MoEfication techniques (Luo et al., 2024;
 149 Gao et al., 2024) replace all linear layers with MoEs. Even greater efficiency is achieved by split-
 150 ting the LoRA adapters into heads (Tian et al., 2024), driving further factorization. MixLoRA (Li
 151 et al., 2024) selectively replaces the QKV matrices in the attention layers with simple LoRAs, while
 152 fusing the MLP layers with parameter-efficient MoEs. More recently, S'MoRE (Zeng et al., 2025)
 153 proposes hierarchical mixtures with structured graphs. We adopt the architecture of MixLoRA, as
 154 it has been shown to be highly effective, and aim to improve the rank efficiency of each adapter.
 155 Moreover, in contrast to S'MoRE, our methods (specifically, SharedLoRA) do not introduce graph
 156 overheads, but make use of a simpler two-tier structure while obtaining SoTA performance.

157

158 **Multiplicative adapters.** Multiplicative adapters for PEFT have seen some adoption, for exam-
 159 ple with Kronecker-Product (Yu et al., 2025). We explore here Matrix product operators (MPOs),
 160 a particularly effective multiplicative decomposition from quantum physics (Pirvu et al., 2010;
 161 Schollwöck, 2011; Orús, 2014). MPOs have been used for compressing linear layers (Gao et al.,
 162 2020) and as a direct alternative to LoRAs (Liu et al., 2021). More similar to this line of work,
 163 MPOE (Gao et al., 2022) also propose an MPO-based approach to parameter-efficient MoEfication.
 164 MPOE decompose the weights using MPO, and then finetune both the auxiliary and the core (only

162 in some steps) tensors. Each expert is then recovered by contracting the shared core tensor with
 163 the specific auxiliary tensors. The key differences between MPOE and our OperA lie in both the
 164 construction of the experts and the routing mechanism. In particular, OperA does not train the core
 165 tensor, making it much more parameter-efficient. Moreover, OperA keeps the residual path as the
 166 shared expert, and fuses the adapters with the weights.
 167

168 3 BACKGROUND

170 **Low-rank adaptation (LoRA).** LoRA is based on low-rank approximations of a matrix. In par-
 171 ticular, given a pretrained weight $W \in \mathbb{R}^{M \times N}$, LoRA consists of two matrices $A \in \mathbb{R}^{M \times r}$ and
 172 $B \in \mathbb{R}^{r \times N}$, with $r \ll M, N$ being the LoRA rank. Crucially, while the LoRA rank places an upper
 173 bound on the dimensionality of the adapter, the actual subspace spanned by the adapter might be
 174 notably smaller. We explore this effect in detail through the use of the *effective rank* in Section 5.4.
 175

176 Next, the product $AB \in \mathbb{R}^{M \times N}$ results in a shape-compatible matrix with W that only requires a
 177 fraction of its parameters to store, producing considerable space savings. This comes to cost of the
 178 rank of AB , which is limited to r , and therefore to its flexibility. The final weight matrix becomes
 then

$$179 \quad W' = W + AB \quad (1)$$

181 **Mixture of experts (MoEs).** MoEs are an architectural design that increases the flexibility and
 182 expressivity of LLMs, while maintaining a constrained increase in the number of parameters. Ex-
 183 perts are matrices $E_1, \dots, E_n \in \mathbb{R}^{M \times N}$ that independently operate on a given input vector $\mathbf{x} \in \mathbb{R}^M$,
 184 factorizing a large representation space into multiple additive components. The most popular imple-
 185 mentation of MoEs uses a noisy top-k routing mechanism that selects k out of n experts for each \mathbf{x} ,
 186 resulting in considerable computational savings at the cost of memory. Specifically, given a router
 187 R

$$188 \quad y = \sum_i^n R(\mathbf{x})_i E_i(\mathbf{x}) \quad (2)$$

190 with

$$191 \quad R(\mathbf{x})_i = \begin{cases} r_i & \text{if expert } i \text{ has been selected} \\ 0 & \text{otherwise} \end{cases} \quad (3)$$

193 and $\sum_i^n r_i = 1$ are the routing weights, usually enforced via a *softmax* operation.
 194

195 **Matrix product operators (MPO).** MPOs, in the setup used in this work, form a multiplicative
 196 representation of an arbitrary matrix $W \in \mathbb{R}^{M \times N}$ into 4D tensors (or cores) with a specific config-
 197 uration. Specifically,

$$198 \quad W = L_1, L_2, \dots, L_n, C, R_1, R_2, \dots, R_n \quad (4)$$

199 with L_i , $i \leq n$ being the left auxiliary cores, C being the center core, and R_i , $i \leq n$ being the right
 200 auxiliary cores. The left and right auxiliary cores are analogous; we will refer to them simply as
 201 auxiliary cores from now on. Therefore, specifying a decomposition with n left (or right) auxiliary
 202 cores results in a total of $2n + 1$ tensors. Each tensor has shape $\mathbb{R}^{d_{in}, r, c, d_{out}}$, with r, c being the
 203 *physical row resp. column legs* and d_{in}, d_{out} being the *bond dimensions*. The specification of r and
 204 c for each core represents the main hyperparameter choice of the MPO system, as we do not restrict
 205 the bond dimensions here (while it is more typical in quantum physics applications; Cui et al. 2015).
 206 Finally, a straightforward tensor contraction of all cores recovers the original matrix.
 207

208 4 RANK-EFFICIENT FINETUNING TECHNIQUES

210 We now present the main contributions of this work, SharedLoRA and OperA. We build both with
 211 the aim of increasing the effective rank, first by improving additive adapters with SharedLoRA,
 212 and then enhancing these adapters with multiplicative interactions with OperA. The two techniques
 213 mainly tackle the building of the experts or adapters to obtain greater rank efficiency at lower pa-
 214 rameters, while we reuse the SoTA combination of LoRA MoEs with LLMs for PEFT found in
 215 MixLoRA (see Appendix B.4 for an ablation of MixLoRA’s fusion). In particular, we replace the
 MLP layers with our MoE adapters and use standard LoRAs for the attention layers.

216 4.1 SHAREDLoRA: TWO-TIER ADDITIVE ADAPTERS
217

218 SharedLoRA uses a combination of two tiers of low-rank adapters to obtain experts with a higher
219 effective rank without impacting the parameter count. Given a weight matrix W and n desired
220 experts, we first initialize n first-tier (or specific) adapters $A_i^s, B_i^s, i \leq n$ of rank r . Next, we
221 initialize g second-tier (or group) adapters $A_i^b, B_i^b, i \leq g$, with g a divisor of n such that $n = g \times m$.
222 We then assign the first group adapters A_1^b, B_1^b to the first m experts, the second group adapters to
223 the second m experts, and so on. Next, each expert E_i is defined as

$$224 \quad E_i = A_i^s B_i^s + A_{i/m}^b B_{i/m}^b \quad (5)$$

226 Together with its noisy top-k router, the input (\mathbf{x}) -dependent SharedLoRA layer becomes

$$227 \quad W' = W + \sum_i^n R(\mathbf{x})_i (A_i^s B_i^s + A_{i/m}^b B_{i/m}^b) \quad (6)$$

230 as is usual in MoEs.

231 Each E_i has a maximum rank of $2r$, for a total number of parameters of $(n + g) \times (M + N) \times r$. In
232 contrast, flat (non-tiered) LoRA MoEs require $2 \times n \times (M + N) \times r$ parameters to achieve the same
233 maximum rank. The two-tier structure results in a $\frac{2n}{n+g} > 1$ (for $g < n$) reduction of parameters at
234 the same rank.

236 4.2 OPERA: QUANTUM-INSPIRED MULTIPLICATIVE ADAPTERS
237

238 OperA leverages multiplicative interactions, which are fundamental to the functioning of deep neu-
239 ral networks (Jayakumar et al., 2020). These interactions are described by MPO, and help OperA
240 achieve an even greater effective rank with lower parameter count compared to SoTA additive
241 adapters. In contrast to LoRA, OperA does not use randomly-initialized fixed-rank adapters, but
242 builds arbitrarily ranked adapters directly from the original weight matrix W . The first step of
243 OperA is to obtain the MPO representation of W using tensor-train singular value decomposition
244 (TT-SVD; Oseledets 2011). Without loss of generality, consider the case of a decomposition into
245 three cores

$$246 \quad W = LCR \quad (7)$$

247 Given n desired experts, we define the multiplicative adapters $L_i, R_i, i \leq n$ by initializing them to
248 equal L, R . Next, each expert E_i becomes

$$249 \quad E_i = L_i C R_i \quad (8)$$

250 with C fixed. Finally, given the same router R as before the input (\mathbf{x}) -dependent OperA layer
251 becomes

$$252 \quad W' = \frac{1}{2} W + \sum_i^n R(\mathbf{x})_i \frac{1}{2} E_i \quad (9)$$

253 with the constant $1/2$ necessary to achieve equality at the beginning of training, analogous to setting
254 the B matrix to 0 in LoRA.

255 The key to the parameter-efficiency of OperA is to concentrate most of the parameters into C , which
256 is not trainable. We remark that the main hyperparameters of TT-SVD consist in the sizes of the
257 *physical legs* r, c of the MPO system. In particular, we set row legs r_1, r_2, r_3 (with $r_1 \times r_2 \times r_3 = M$)
258 and column legs c_1, c_2, c_3 (with $c_1 \times c_2 \times c_3 = N$). With these parameters set, we can now fully
259 describe the shapes of the MPO:

- 260 • $L \in \mathbb{R}^{1 \times r_1 \times c_1 \times d_1}$
- 261 • $C \in \mathbb{R}^{d_1 \times r_2 \times c_2 \times d_2}$
- 262 • $R \in \mathbb{R}^{d_2 \times r_3 \times c_3 \times 1}$

263 The bond dimensions d_1, d_2 are an effect of TT-SVD and cannot be directly controlled, except by
264 cutting the least-relevant singular values, which would result in a lossy reconstruction of W as in
265 regular SVD. Therefore, we can simply choose $r_2 \gg r_{i \neq 2}$ and $c_2 \gg c_{i \neq 2}$ to obtain the desired
266 effect.

270 The multiplicative adapters L_i, R_i do not directly limit the rank of the expert, allowing the system
 271 to exhibit greater variety and flexibility. Nonetheless, the greater parameter efficiency comes at a
 272 computational cost, as each expert is now full-rank and must be obtained from a tensor contraction
 273 at every step. Therefore, OperA can be seen as a compute-bound but memory-efficient alternative
 274 to LoRA adapters, which is highly beneficial for common GPU implementations where compute is
 275 abundant and memory bandwidth is often the principal bottleneck.

277 5 RESULTS

279 Here we report the results of our evaluation, including all relevant ablations for the different param-
 280 eters of both SharedLoRA and OperA.

282 5.1 EXPERIMENTAL SETUP

284 **Models.** We compare MixLoRA, SharedLoRA, and OperA on a variety of models to ensure
 285 the consistency of our performance results. From Meta, we test: Llama3-8B, Llama3.1-8B, and
 286 Llama3.2-3B. From Qwen, we test: Qwen2.5-3B, and Qwen2.5-7B. Finally, from Microsoft we test
 287 Phi4-14B. This choice of 6 models covers a representative range of sizes (from 3B to 14B parame-
 288 ters) and of model origins.

289 **Tasks.** We evaluate our work on multiple datasets and tasks with varying size and complexity. For
 290 each dataset, we first finetune each adapter on the training split, and then evaluate the accuracy on
 291 the testing split. The task ensemble consists of question-and-answer tasks (ARC-e, ARC-c, PIQA,
 292 OpenBookQA), classification tasks (BoolQ), and completion tasks (HellaSwag, Winogrande). All
 293 tasks are evaluated on accuracy.

295 **MoEs.** For all experiments, we use 8 total experts with 2 active experts per token. Following best
 296 practices, we use noisy top-k routing with an auxiliary router balancing loss.

298 **LoRA.** For both LoRA based approaches, MixLoRA and SharedLoRA, the rank of the adapters
 299 is the main hyperparameter. For MixLoRA, the rank is set to either 16 (original, see Section 5.2) or
 300 12 (optimal, see Appendix B.1). For SharedLoRA, we match and surpass the parameter efficiency
 301 of MixLoRA with ranks of either 12 or 8.

303 **MPO.** MPOs, as used in this work, do not have rank. We instead focus on the sizes of the physical
 304 legs to achieve the desired parameter efficiency. The sizes are specific to each model, and can be
 305 found in Appendix A. In OperA, we also use simple LoRA for the QKV matrices in the attention
 306 components, and fix the rank to 6 to give enough flexibility for adaptation without contributing a
 307 large amount of parameters. Therefore, most of the finetuning is left to the multiplicative adapters.

308 **Environment.** All experiments are performed on Nvidia A100 80GB using PyTorch 2.6 and the
 309 MoE-PEFT (Li et al., 2024) codebase. All models are trained using mixed fp32 and bf16.

312 5.2 BASELINE

313 We replicate the setup of MixLoRA to obtain comparable results with the current SoTA, and follow
 314 the original hyperparameter selection which found rank 16 to be optimal. In Table 1 we show
 315 that SharedLoRA equals or surpasses the baseline with a smaller rank (12 vs 16), leading to 7.1%
 316 average parameter savings. At the same time, OperA at SoTA accuracy achieves on average a 36%
 317 space saving across all tested models. Overall, SharedLoRA and OperA surpass the baseline on all
 318 the models tested, with notable parameter efficiency gains (see Appendix A for the configuration of
 319 each adapter).

321 5.3 FIXED PARAMETER BUDGET

323 We have demonstrated that SharedLoRA and OperA are competitive with the SoTA while requiring
 notably less parameters. At the same time, in Appendix B.1 we also further optimize MixLoRA

324
 325 **Table 1: Accuracy of MixLoRA, and our SharedLoRA and OperA.** For each model, we report
 326 the reduction in parameters over MixLoRA and the task accuracy. The baseline parameter count is
 327 taken as MixLoRA with rank 16.

Model	Adapter	% redux ↓	ARC-c ↑	ARC-e ↑	PIQA ↑	OBQA ↑	BoolQ ↑	HS ↑	WG ↑	Avg ↑
Llama3-8B	MixLoRA	-0.0	75.76	87.08	86.18	89.00	73.61	94.63	83.11	84.20
	SharedLoRA	-0.0	75.51	86.28	86.02	86.60	74.13	94.03	82.79	83.62
	OperA	-0.0	77.39	86.28	88.30	87.60	76.36	96.15	81.45	84.79
Llama3.1-8B	MixLoRA	-0.0	76.96	86.82	86.40	83.20	74.65	94.77	84.14	83.85
	SharedLoRA	-7.1	76.11	87.21	86.18	83.00	74.43	94.52	83.74	83.60
	OperA	-28.2	76.88	86.32	87.92	85.20	75.23	96.10	80.58	84.03
Llama3.2-3B	MixLoRA	-0.0	68.26	83.12	83.02	77.40	71.50	92.13	75.14	78.65
	SharedLoRA	-7.6	69.28	83.29	84.00	79.00	72.20	91.70	76.72	79.46
	OperA	-29.8	66.98	81.73	83.19	77.20	70.98	92.93	74.19	78.17
Phi4-14B	MixLoRA	-0.0	91.21	94.28	91.90	92.60	75.47	95.95	88.79	90.03
	SharedLoRA	-6.5	90.36	95.20	92.44	92.00	76.18	96.12	88.32	90.09
	OperA	-45.8	88.14	92.84	91.84	91.00	74.49	95.25	86.27	87.43
Qwen2.5-3B	MixLoRA	-0.0	80.12	88.64	86.62	87.60	70.92	91.67	80.03	83.66
	SharedLoRA	-6.9	79.95	88.05	86.23	87.40	71.47	91.96	81.21	83.75
	OperA	-60.6	80.89	89.40	86.02	87.60	70.06	92.99	74.82	83.11
Qwen2.5-7B	MixLoRA	-0.0	87.88	94.19	88.74	92.80	74.52	95.29	83.27	88.10
	SharedLoRA	-7.1	87.03	92.04	88.36	92.20	74.43	94.85	85.16	87.72
	OperA	-24.1	87.71	93.39	90.42	91.40	74.74	95.91	83.66	88.18

348 both for accuracy and for parameter count, and show that SharedLoRA and OperA outperform
 349 SoTA in this setting as well. However, the question remains whether OperA can actually leverage
 350 its multiplicative interactions to be more parameter-efficient than the baseline. Table 2 indicates that
 351 OperA is Pareto-optimal on 5 out of the 6 models, achieving higher accuracy at a lower parameter
 352 count than the baseline. Phi4 is the only exception, possibly due to its greater size which hampers
 353 convergence.

354
 355 **Table 2: Comparison of MixLoRA and OperA given the same parameter budget.** For each
 356 model, we report the reduction in parameters over MixLoRA and the task accuracy. The baseline
 357 parameter count is taken as MixLoRA with rank 16.

Model	Adapter	% redux ↓	ARC-c ↑	ARC-e ↑	PIQA ↑	OBQA ↑	BoolQ ↑	HS ↑	WG ↑	Avg ↑
Llama3-8B	MixLoRA	-56.0%	78.75	87.12	83.81	85.20	74.62	94.75	83.90	84.02
	OperA	-60.6%	77.64	86.41	87.60	84.20	74.74	95.71	83.03	84.19
Llama3.1-8B	MixLoRA	-56.0%	78.33	86.45	83.60	87.40	75.69	95.16	83.42	84.29
	OperA	-60.6%	77.73	87.29	88.19	85.40	75.69	95.91	80.03	84.75
Llama3.2-3B	MixLoRA	-55.7%	69.33	83.42	83.17	79.40	70.98	92.15	76.64	79.30
	OperA	-55.0%	69.08	84.64	82.64	79.40	71.53	93.60	75.16	79.44
Phi4-14B	MixLoRA	-71.4%	91.47	96.68	92.27	93.60	76.02	95.81	87.85	90.53
	OperA	-45.8%	88.14	92.84	91.84	91.00	74.49	95.38	87.21	88.54
Qwen2.5-3B	MixLoRA	-55.9%	82.08	88.39	85.70	84.93	70.80	92.76	79.79	83.49
	OperA	-60.6%	80.89	89.40	86.02	87.60	70.06	92.99	77.82	83.54
Qwen2.5-7B	MixLoRA	-56.1%	86.77	91.92	88.93	92.40	75.17	95.36	85.79	88.05
	OperA	-63.2%	87.63	92.51	90.59	94.00	74.07	95.76	83.98	88.36

374 5.4 EFFECTIVE RANK

375
 376 While the LoRA rank puts an upper bound to the dimensionality of the PEFT, whether the adapters
 377 do actually make use of all available space can be directly investigated. Here, we choose the effective
 rank (Roy & Vetterli, 2007) as the measure of interest due to its inherent robustness. The effective

rank is the measure of the entropy of the singular values of a matrix, computed as:

$$\text{erank}(W) = \frac{\|W\|_F^2}{\|W\|_2^2} \quad (10)$$

where $\|\cdot\|_F$ is the Frobenius norm and $\|\cdot\|_2$ is the L2 norm. The effective rank computes the ratio between the sum of all singular values to the greatest one, quantifying the concentration of the singular values and therefore the effective dimensionality of the matrix.

We compute the effective rank of both MixLoRA and SharedLoRA adapters as training progresses as the effective rank of the full LoRA matrix, i.e. $\text{erank}(E_i)$. In the case of OperA, we compute the effective rank of $W - E_i$ instead, as each E_i is always full rank and we wish to evaluate the additional dimensionality brought by E_i to the system, rather than its raw dimensionality.

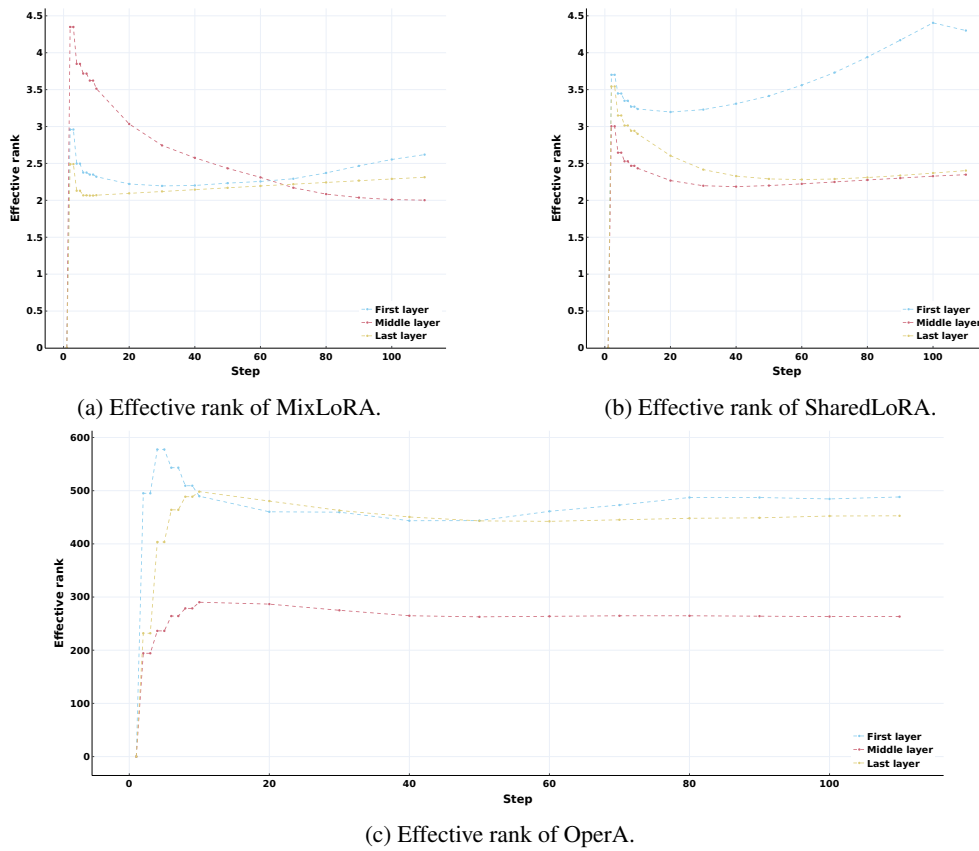


Figure 2: **Effective rank of the adapters.** Development of the effective rank as finetuning progresses.

Figure 2 shows that the effective rank quickly rises at the beginning of training, as expected, but then progressively settles. In the case of MixLoRA, the effective rank degrades quickly, hovering around 2.5 for both shallow and deep layers, consistent with the findings in Li et al. (2024) that performance is maintained down to a LoRA rank of 2. On the other hand, the effective rank of SharedLoRA remains notably higher, especially in the first layer, surpassing 4. This indicates both that SharedLoRA achieves a higher effective rank, and also that it places more emphasis on shallower layers, closer to the input. Finally, OperA's effective rank is notably higher and more stable than the additive approaches, indicating that the additional information gained by OperA spans a much greater subspace even with fewer parameters.

5.5 ABLATIONS

Optimal rank. The main hyperparameter that determines the parameter count of LoRA-based approaches is the rank of the adapters. As mentioned earlier, to obtain baseline results we first apply

MixLoRA with rank 16, found to be optimal in the original work. However, we also perform a more fine-grained search using more modern architectures to ensure as strong a baseline as possible. Fig. 3 shows that performance peaks at rank 12 for Llama3-8B, while it remains stable after rank 12 for Qwen2.5-3B. Therefore, we choose rank 12 as the most parameter-efficient solution for both, and extend this evaluation to all architectures to establish an optimized MixLoRA baseline in Appendix B.1.

Optimal MPO size. The parameter count of OperA is mainly determined by the configuration of the physical legs, which are specific to each model and are evaluated empirically for effectiveness. Nonetheless, the amount of legs also contributes to the downstream performance by varying the degree of factorization. To obtain the optimal number, we sweep from 3 to 7 legs on Qwen2.5-3B and check the average performance across 5 tasks. Figure 2c shows that 5 legs provides the best accuracy.

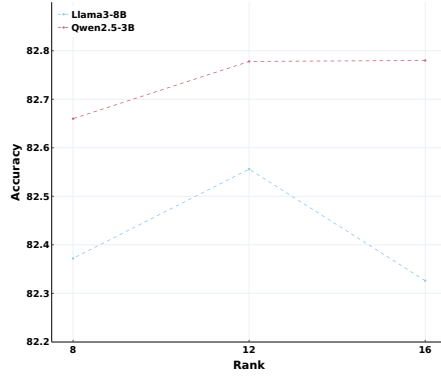


Figure 3: **MixLoRA performance depends on rank.** We report the average accuracy of Llama3-8B and Qwen2.5-3B at varying LoRA ranks, using MixLoRA.

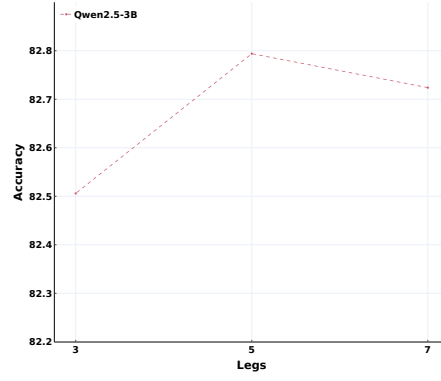


Figure 4: **OperA performance depends on the number of legs.** We report the average accuracy of Qwen2.5-3B at various leg configurations, using OperA.

6 CONCLUSION

In this work, we present SharedLoRA and OperA, two rank-efficient techniques for PEFT MoEification. SharedLoRA is a two-tiered structure of LoRA adapters, which makes use of the more conventional additive interactions. This structure allows SharedLoRA to achieve higher performance at lower parameter counts, by achieving a higher effective rank than the SoTA. OperA, instead, is built on multiplicative interactions, which are fundamental to learning in deep neural networks (Jayakumar et al., 2020). OperA leverages MPOs, a multiplicative decomposition stemming from quantum physics, to produce low-parameter adapters which can be combined with the pretrained weights to obtain powerful high-rank experts. Therefore, we highlight the usefulness of the effective rank as a quantification of the dimensionality of an adapter, and show that targeting it leads to improved performance without an increase in parameter count.

Overall, we show that SharedLoRA and OperA reach SoTA results on most of the models and tasks tested. Specifically, OperA reaches a higher accuracy than the baseline at a lower parameter cost on 5 out of the 6 models tested, making it the optimal choice for a given parameter budget.

Further work is necessary to evaluate the impact of structured compositions of LoRAs, such as our two-tier SharedLoRA and the graph-based S'MoRE Zeng et al. (2025). At the same time, multiplicative adapters Yu et al. (2025) have shown significant promise to replace additive adapters such as LoRA in some situations, with our OperA achieving optimal performance across the board. However, the level of optimization that contributes to the success of LoRA has not yet been achieved for its multiplicative alternatives, and is a significant avenue for future research.

486 ETHICS STATEMENT

487

488 This work does not involve human subjects, personally identifiable information, or sensitive data.
 489 All experiments were conducted using publicly available models and datasets. Our focus on improv-
 490 ing model performance in low-compute budget environments was a central consideration to mitigate
 491 environmental impact. The authors declare no known conflicts of interest.

492

493 REPRODUCIBILITY STATEMENT

494

495 This paper describes the proposed SharedLoRA and OperA techniques, including the details of the
 496 algorithms in Section 4 and the experimental setup in Section 5.1.

497

The hyperparameters for all the models evaluated can be found in Appendix A.

498

499 The code is provided in the supplementary materials, along with the required experimental environ-
 500 ments.

500

501

502 REFERENCES

503

504 Marah Abdin, Jyoti Aneja, Harkirat Behl, Sébastien Bubeck, Ronen Eldan, Suriya Gunasekar,
 505 Michael Harrison, Russell J. Hewett, Mojan Javaheripi, Piero Kauffmann, James R. Lee, Yin Tat
 506 Lee, Yuanzhi Li, Weishung Liu, Caio C. T. Mendes, Anh Nguyen, Eric Price, Gustavo de Rosa,
 507 Olli Saarikivi, Adil Salim, Shital Shah, Xin Wang, Rachel Ward, Yue Wu, Dingli Yu, Cyril Zhang,
 508 and Yi Zhang. Phi-4 technical report. *arXiv preprint arXiv:2412.08905*, 2024.

509

510 Yonatan Bisk, Rowan Zellers, Ronan Le Bras, Jianfeng Gao, and Yejin Choi. PIQA: Reasoning
 511 about physical commonsense in natural language. In *AAAI*, 2020.

512

513 Christopher Clark, Kenton Lee, Ming-Wei Chang, Tom Kwiatkowski, Michael Collins, and Kristina
 514 Toutanova. BoolQ: Exploring the surprising difficulty of natural yes/no questions. In *NAACL*,
 515 2019.

516

517 Peter Clark, Isaac Cowhey, Oren Etzioni, Tushar Khot, Ashish Sabharwal, Carissa Schoenick, and
 518 Oyvind Tafjord. Think you have solved question answering? try ARC, the AI2 reasoning chal-
 519 lenge. *arXiv preprint arXiv:1803.05457v1*, 2018.

520

521 Jian Cui, J. Ignacio Cirac, and Mari Carmen Bañuls. Variational matrix product operators for the
 522 steady state of dissipative quantum systems. *Phys. Rev. Lett.*, 114, 2015.

523

524 DeepSeek-AI. DeepSeek-V3 technical report. *arXiv preprint arXiv:2412.19437*, 2025.

525

526 Tim Dettmers, Artidoro Pagnoni, Ari Holtzman, and Luke Zettlemoyer. QLoRA: Efficient finetuning
 527 of quantized LLMs. In *NeurIPS*, 2023.

528

529 Shihan Dou, Enyu Zhou, Yan Liu, Songyang Gao, Wei Shen, Limao Xiong, Yuhao Zhou, Xiao
 530 Wang, Zhiheng Xi, Xiaoran Fan, Shiliang Pu, Jiang Zhu, Rui Zheng, Tao Gui, Qi Zhang, and
 531 Xuanjing Huang. LoRAMoE: Alleviating world knowledge forgetting in large language models
 532 via MoE-style plugin. In *Proceedings of the Association for Computational Linguistics (ACL)*,
 533 2024.

534

535 William Fedus, Barret Zoph, and Noam Shazeer. Switch transformers: Scaling to trillion parameter
 536 models with simple and efficient sparsity. *Journal of Machine Learning Research (JMLR)*, 23
 537 (120):1–39, 2022.

538

539 Wenfeng Feng, Chuzhan Hao, Yuewei Zhang, Yu Han, and Hao Wang. Mixture-of-loras: An effi-
 540 cient multitask tuning method for large language models. In *International Conference on Com-
 541 putational Linguistics, Language Resources and Evaluation (LREC-COLING)*, 2024.

542

543 Chongyang Gao, Kezhen Chen, Jinmeng Rao, Baochen Sun, Ruibo Liu, Daiyi Peng, Yawen Zhang,
 544 Xiaoyuan Guo, Jie Yang, and VS Subrahmanian. Higher layers need more LoRA experts. *arXiv*
 545 preprint *arXiv:2402.08562*, 2024.

540 Ze-Feng Gao, Song Cheng, Rong-Qiang He, Z. Y. Xie, Hui-Hai Zhao, Zhong-Yi Lu, and Tao Xiang.
 541 Compressing deep neural networks by matrix product operators. *Physical Review Research*, 2(2),
 542 2020.

543 Ze-Feng Gao, Peiyu Liu, Wayne Xin Zhao, Zhong-Yi Lu, and Ji-Rong Wen. Parameter-efficient
 544 mixture-of-experts architecture for pre-trained language models. In *International Conference on*
 545 *Computational Linguistics (ICCL)*, 2022.

546 Zeyu Han, Chao Gao, Jinyang Liu, Jeff Zhang, and Sai Qian Zhang. Parameter-efficient fine-tuning
 547 for large models: A comprehensive survey. *Transactions on Machine Learning Research (TMLR)*,
 548 2024.

549 Soufiane Hayou, Nikhil Ghosh, and Bin Yu. PLoP: Precise LoRA placement for efficient finetuning
 550 of large models. *arXiv preprint arXiv:2506.20629*, 2025.

551 Edward J Hu, yelong shen, Phillip Wallis, Zeyuan Allen-Zhu, Yuanzhi Li, Shean Wang, Lu Wang,
 552 and Weizhu Chen. LoRA: Low-rank adaptation of large language models. In *ICLR*, 2022.

553 IBM. Granite 3.0 language models. <https://github.com/ibm-granite/granite-3.0-language-models/>, 2024.

554 Siddhant M. Jayakumar, Wojciech M. Czarnecki, Jacob Menick, Jonathan Schwarz, Jack Rae, Si-
 555 mon Osindero, Yee Whye Teh, Tim Harley, and Razvan Pascanu. Multiplicative interactions and
 556 where to find them. In *ICLR*, 2020.

557 Albert Q. Jiang, Alexandre Sablayrolles, Antoine Roux, Arthur Mensch, Blanche Savary, Chris
 558 Bamford, Devendra Singh Chaplot, Diego de las Casas, Emma Bou Hanna, Florian Bressand, Gi-
 559 anna Lengyel, Guillaume Bour, Guillaume Lample, Lélio Renard Lavaud, Lucile Saulnier, Marie-
 560 Anne Lachaux, Pierre Stock, Sandeep Subramanian, Sophia Yang, Szymon Antoniak, Teven Le
 561 Scao, Théophile Gervet, Thibaut Lavril, Thomas Wang, Timothée Lacroix, and William El Sayed.
 562 Mixtral of experts. *arXiv preprint arXiv:2401.04088*, 2024.

563 Dawid Jan Kopiczko, Tijmen Blankevoort, and Yuki M Asano. VeRA: Vector-based random matrix
 564 adaptation. In *ICLR*, 2024.

565 Bo Li, Yifei Shen, Jingkang Yang, Yezhen Wang, Jiawei Ren, Tong Che, Jun Zhang, and Ziwei Liu.
 566 Sparse mixture-of-experts are domain generalizable learners. In *ICLR*, 2023.

567 Dengchun Li, Yingzi Ma, Naizheng Wang, Zhengmao Ye, Zhiyuan Cheng, Yinghao Tang, Yan
 568 Zhang, Lei Duan, Jie Zuo, Cal Yang, and Mingjie Tang. MixLoRA: Enhancing large language
 569 models fine-tuning with LoRA-based mixture of experts. *arXiv preprint arXiv:2404.15159*, 2024.

570 Haotian Liu, Chunyuan Li, Qingyang Wu, and Yong Jae Lee. Visual instruction tuning. In *NeurIPS*,
 571 2023.

572 Haotian Liu, Chunyuan Li, Yuheng Li, Bo Li, Yuanhan Zhang, Sheng Shen, and Yong Jae Lee.
 573 LLaVA-NeXT: Improved reasoning, OCR, and world knowledge, January 2024a. URL <https://llava-vl.github.io/blog/2024-01-30-llava-next/>.

574 Peiyu Liu, Ze-Feng Gao, Wayne Xin Zhao, Zhi-Yuan Xie, Zhong-Yi Lu, and Ji-Rong Wen. Enabling
 575 lightweight fine-tuning for pre-trained language model compression based on matrix product op-
 576 erators. In *International Joint Conference on Natural Language Processing (IJCNLP)*, 2021.

577 Shih-Yang Liu, Chien-Yi Wang, Hongxu Yin, Pavlo Molchanov, Yu-Chiang Frank Wang, Kwang-
 578 Ting Cheng, and Min-Hung Chen. DoRA: Weight-decomposed low-rank adaptation. In *ICML*,
 579 2024b.

580 Tongxu Luo, Jiahe Lei, Fangyu Lei, Weihao Liu, Shizhu He, Jun Zhao, and Kang Liu. MoELoRA:
 581 Contrastive learning guided mixture of experts on parameter-efficient fine-tuning for large lan-
 582 guage models. *arXiv preprint arXiv:2402.12851*, 2024.

583 Meta AI. The Llama 3 herd of models. *arXiv preprint arXiv:2407.21783*, 2024.

594 Todor Mihaylov, Peter Clark, Tushar Khot, and Ashish Sabharwal. Can a suit of armor conduct
 595 electricity? a new dataset for open book question answering. In *EMNLP*, 2018.
 596

597 OpenAI. Gpt-4 technical report. *arXiv preprint arXiv:2303.08774*, 2024.
 598

599 OpenAI. GPT-5 system card. <https://openai.com/index/gpt-5-system-card/>,
 600 2025.

601 Román Orús. A practical introduction to tensor networks: Matrix product states and projected
 602 entangled pair states. *Annals of physics*, 349:117–158, 2014.
 603

604 I. V. Oseledets. Tensor-Train decomposition. *SIAM Journal on Scientific Computing*, 33(5):2295–
 605 2317, 2011.

606 Venkatesh Balavadhani Parthasarathy, Ahtsham Zafar, Aafaq Khan, and Arsalan Shahid. The ul-
 607 timate guide to fine-tuning LLMs from basics to breakthroughs: An exhaustive review of tech-
 608 nologies, research, best practices, applied research challenges and opportunities. *arXiv preprint*
 609 *arXiv:2408.13296*, 2024.
 610

611 Bogdan Pirvu, Valentin Murg, J Ignacio Cirac, and Frank Verstraete. Matrix product operator rep-
 612 resentations. *New Journal of Physics*, 12(2), 2010.

613 Joan Puigcerver, Carlos Riquelme Ruiz, Basil Mustafa, and Neil Houlsby. From sparse to soft
 614 mixtures of experts. In *ICLR*, 2024.
 615

616 Qwen AI. Qwen3-Next. [https://qwen.ai/blog?id=](https://qwen.ai/blog?id=4074cca80393150c248e508aa62983f9cb7d27cd&from=research)
 617 4074cca80393150c248e508aa62983f9cb7d27cd&from=research.
 618 latest-advancements-list, 2025a.

619 Qwen AI. Qwen2.5 technical report. *arXiv preprint arXiv:2412.15115*, 2025b.
 620

621 Adithya Renduchintala, Tugrul Konuk, and Oleksii Kuchaiev. Tied-LoRA: Enhancing parameter
 622 efficiency of LoRA with weight tying. In *NAACL*, 2024.
 623

624 Olivier Roy and Martin Vetterli. The effective rank: A measure of effective dimensionality. In
 625 *European signal processing conference*, 2007.

626 Carlos Riquelme Ruiz, Joan Puigcerver, Basil Mustafa, Maxim Neumann, Rodolphe Jenatton,
 627 André Susano Pinto, Daniel Keysers, and Neil Houlsby. Scaling vision with sparse mixture of
 628 experts. In *NeurIPS*, 2021.
 629

630 Keisuke Sakaguchi, Ronan Le Bras, Chandra Bhagavatula, and Yejin Choi. Winogrande: an adver-
 631 sarial winograd schema challenge at scale. *Communications ACM*, 64(9):99–106, 2021.
 632

633 Ulrich Schollwöck. The density-matrix renormalization group in the age of matrix product states.
 634 *Annals of physics*, 326(1):96–192, 2011.

635 Noam Shazeer, Azalia Mirhoseini, Krzysztof Maziarz, Andy Davis, Quoc Le, Geoffrey Hinton, and
 636 Jeff Dean. Outrageously large neural networks: The sparsely-gated mixture-of-experts layer. In
 637 *ICLR*, 2017.
 638

639 Chunlin Tian, Zhan Shi, Zhijiang Guo, Li Li, and Cheng zhong Xu. HydraloRA: An asymmetric
 640 loRA architecture for efficient fine-tuning. In *NeurIPS*, 2024.

641 Jiaqi Wang, Hanqi Jiang, Yiheng Liu, Chong Ma, Xu Zhang, Yi Pan, Mengyuan Liu, Peiran Gu,
 642 Sichen Xia, Wenjun Li, Yutong Zhang, Zihao Wu, Zhengliang Liu, Tianyang Zhong, Bao Ge,
 643 Tuo Zhang, Ning Qiang, Xintao Hu, Xi Jiang, Xin Zhang, Wei Zhang, Dinggang Shen, Tianming
 644 Liu, and Shu Zhang. A comprehensive review of multimodal large language models: Performance
 645 and challenges across different tasks. *arXiv preprint arXiv:2408.01319*, 2024.
 646

647 Yifei Xia, Fangcheng Fu, Wentao Zhang, Jiawei Jiang, and Bin CUI. Efficient multi-task LLM
 648 quantization and serving for multiple LoRA adapters. In *NeurIPS*, 2024a.

648 Yuchen Xia, Jiho Kim, Yuhang Chen, Haojie Ye, Souvik Kundu, Cong Hao, and Nishil Talati.
649 Understanding the performance and estimating the cost of LLM fine-tuning. *arXiv preprint*
650 *arXiv:2408.04693*, 2024b.

651 Jiahui Yang, Yongjia Ma, Donglin Di, Hao Li, Wei Chen, Yan Xie, Jianxun Cui, Xun Yang, and
652 Wangmeng Zuo. QR-LoRA: Efficient and disentangled fine-tuning via QR decomposition for
653 customized generation. *arXiv preprint arXiv:2507.04599*, 2025.

654 Beiming Yu, Zhenfei Yang, and Xiushuang Yi. MoKA: Parameter efficiency fine-tuning via mix-
655 ture of Kronecker product adaption. In *International Conference on Computational Linguistics*
656 (*ICCL*), 2025.

657 Tongtian Yue, Longteng Guo, Jie Cheng, Xuan Gao, Hua Huang, and Jing Liu. Ada-K routing:
658 Boosting the efficiency of MoE-based LLMs. In *ICLR*, 2025.

659 Rowan Zellers, Ari Holtzman, Yonatan Bisk, Ali Farhadi, and Yejin Choi. HellaSwag: Can a
660 machine really finish your sentence? In *Proceedings of the Association for Computational Lin-*
661 *guistics*, 2019.

662 Hanqing Zeng, Yinglong Xia, Zhuokai Zhao, Gilbert Jiang, Qiang Zhang, Jiayi Liu, Lizhu Zhang,
663 Xiangjun Fan, and Benyu Zhang. S'more: Structural mixture of residual experts for llm fine-
664 tuning. *arXiv preprint arXiv:2504.06426*, 2025.

665

666

667

668

669

670

671

672

673

674

675

676

677

678

679

680

681

682

683

684

685

686

687

688

689

690

691

692

693

694

695

696

697

698

699

700

701

702 A ADAPTER DETAILS
703
704
705
706707 A.1 MIXLORA
708709 We report the hyperparameters chosen for MixLoRA in Table 3. The hyperparameters are chosen
710 based on the findings in the original paper, and then further finetuning as described in this work.
711712 Table 3
713

714 Model	715 Rank	716 Alpha	717 Dropout	718 Results
All	16	32	0.05	Section 5.2
All	12	24	0.05	Appendix B.1
All	8	16	0.05	Section 5.5
All	7	14	0.05	Section 5.4

720 A.2 SHAREDLoRA
721722 We report the hyperparameters chosen for SharedLoRA in Table 3. The hyperparameters are chosen
723 based on an search conducted on the rank and dropout ratio.
724725 Table 4
726

727 Model	728 Rank	729 Alpha	730 Dropout	731 Results
All	12	24	0.2	Section 5.2
All	8	16	0.2	Appendix B.1

732 A.3 OPERA
733734 The hyperparameters for OperA depend on the chosen model, specifically the size of the physical
735 legs. We report in Table 5 both the row legs (Row) and the column legs (Column) in the format
736 $r_1 : r_2 : \dots : r_l$ and $c_1 : c_2 : \dots : c_l$, with l the number of legs. The number of legs here is always 5,
737 as found in Section 5.5.
738
739
740
741
742
743
744
745
746
747
748
749
750
751
752
753
754
755

756
 757
 758
 759
 760
 761
 762
 763
 764
 765
 766
 767
 768
 769
 770
 771
 772
 773
 774

Table 5

Model	Column	Row	Rank	Alpha	Dropout	Results
Llama3-8B	2:8:32:4:2	4:7:32:4:4	6	12	0.2	Section 5.2
	2:8:32:4:2	4:7:32:4:4	6	12	0.2	Section 5.4, 5.5, Appendix B.1
Llama3.1-8B	2:8:32:4:2	4:7:32:4:4	6	12	0.2	Section 5.2
	2:8:32:4:2	4:7:32:4:4	6	12	0.2	Section 5.4, 5.5, Appendix B.1
Llama3.2-3B	2:8:12:8:2	2:8:32:8:2	6	12	0.2	Section 5.2
	2:8:12:8:2	2:8:32:8:2	6	12	0.2	Section 5.4, 5.5, Appendix B.1
Phi4-14B	2:8:40:4:2	4:8:35:4:4	6	12	0.2	Section 5.2
	2:8:40:4:2	4:8:35:4:4	6	12	0.2	Section 5.4, 5.5, Appendix B.1
Qwen2.5-3B	2:8:16:4:2	2:8:43:8:2	6	12	0.2	Section 5.2
	2:8:16:4:2	2:8:43:8:2	6	12	0.2	Section 5.4, 5.5, Appendix B.1
Qwen2.5-7B	2:8:28:4:2	4:8:37:8:2	6	12	0.2	Section 5.2
	2:8:28:4:2	4:8:37:8:2	6	12	0.2	Section 5.4, 5.5, Appendix B.1

792
 793
 794
 795
 796
 797
 798
 799
 800
 801
 802
 803
 804
 805
 806
 807
 808
 809

810
811 **B ADDITIONAL RESULTS**812 **B.1 RANK OPTIMIZATION**813
814 We perform an hyperparameter search on Llama3-8B and Qwen2.5-3B to obtain the optimal rank
815 of MixLoRA on more recent architectures. Our rank sweep is more fine grained than in the original
816 work, and our results indicate that substantial space savings can be achieved with rank 12 (see
817 Section 5.4 for the ablation results). Therefore, we also aim to reduce the parameters of the MoEs
818 in SharedLoRA and OperA. The results in Table 6 indicate that both our methods are stable and
819 amenable to different configurations, providing evidence for their flexibility. This is especially re-
820 markable for OperA, which shows similar robustness to an already established method such as LoRA
821 while employing a notably different technique. Specifically, the performance of SharedLoRA and
822 OperA in Table 6 are again equal or superior to MixLoRA, with even more impressive space savings
823 of 38% and 58% respectively over the original baseline.824
825 **Table 6: Accuracy of rank-optimized MixLoRA, SharedLoRA, and OperA.** For each model, we
826 report the reduction in parameters over MixLoRA and the task accuracy. The baseline parameter
827 count is taken as MixLoRA with rank 16.828
829

Model	Adapter	% redux ↓	ARC-c ↑	ARC-e ↑	PIQA ↑	OBQA ↑	BoolQ ↑	HS ↑	WG ↑	Avg ↑
Llama3-8B	MixLoRA	-24.9	77.13	87.84	85.90	87.20	74.71	94.70	83.35	84.40
	SharedLoRA	-38.2	78.92	86.24	86.02	86.60	74.13	94.92	83.19	84.29
	OperA	-60.6	77.64	86.41	87.60	84.20	74.74	95.71	83.03	84.19
Llama3.1-8B	MixLoRA	-24.9	76.11	85.27	87.76	84.20	75.50	94.93	84.61	84.05
	SharedLoRA	-38.2	76.62	87.46	86.62	86.60	74.65	94.92	84.29	84.45
	OperA	-60.6	77.73	87.29	88.19	85.40	75.69	95.91	83.03	84.75
Llama3.2-3B	MixLoRA	-25.2	69.28	84.85	83.57	79.80	72.20	92.53	73.09	79.33
	SharedLoRA	-38.2	68.00	82.66	83.79	79.00	72.20	92.87	76.24	79.25
	OperA	-55.0	69.08	84.64	82.64	79.40	71.53	93.60	75.16	79.44
Phi4-14B	MixLoRA	-25.0	90.36	96.84	91.89	94.00	75.41	95.81	88.32	90.38
	SharedLoRA	-37.8	90.87	95.70	91.78	91.80	75.72	96.01	88.08	89.99
	OperA	-71.4	88.14	92.84	91.84	91.00	74.49	95.38	87.21	88.54
Qwen2.5-3B	MixLoRA	-25.0	81.06	88.59	86.56	86.40	71.28	91.94	79.08	83.56
	SharedLoRA	-37.8	81.57	89.31	85.96	87.60	71.56	92.16	79.32	83.93
	OperA	-60.6	80.89	89.40	86.02	87.60	70.06	92.99	77.82	83.54
Qwen2.5-7B	MixLoRA	-24.9	87.54	92.17	88.90	92.80	74.10	95.60	84.14	87.89
	SharedLoRA	-37.9	87.03	91.54	89.99	92.20	73.90	95.10	84.14	87.56
	OperA	-63.2	87.63	92.51	90.59	94.00	74.07	95.76	83.98	88.36

849 **B.2 RANK ABLATION**850
851 Table 7 report all the results of the rank ablation performed on Qwen2.5-3B and Llama3-7B.852
853 **Table 7: Results of the rank ablation.** We sweep the rank of MixLoRA from 16 to 8 on Qwen2.5-
854 3B and Llama3-8B, to determine the optimal configuration.855
856

Adapter	Model	Rank ↓	% redux ↓	ARC-c ↑	ARC-e ↑	PIQA ↑	OBQA ↑	BoolQ ↑	Avg ↑
MixLoRA	Qwen2.5-3B	16	-0%	80.12	88.64	86.62	87.60	70.92	82.78
		12	-24.5%	81.06	88.59	86.56	86.40	71.28	82.78
		8	-49.5%	81.91	89.01	83.19	87.60	71.59	82.66
	Llama3-8B	16	-0%	75.76	87.08	86.18	89.00	73.61	82.33
		12	-24.9%	77.13	87.84	85.90	87.20	74.71	82.56
		8	-49.8%	78.84	87.33	83.59	86.80	75.30	82.37

864 B.3 MPO SIZE ABLATION
865866 Table 8 report all the results of the ablation on the number of legs of the MPO performed on
867 Qwen2.5-3B.868 Table 8: **Results of the MPO size ablation.** We sweep the number of legs in OperA from 3 to 7 on
869 Qwen2.5-3B, to determine the optimal configuration.
870

Adapter	Model	Column	Row	% redux ↓	ARC-c ↑	ARC-e ↑	PIQA ↑	OBQA ↑	BoolQ ↑	Avg ↑
OperA	Qwen2.5-3B	2:2:4:16:2:2	2:2:4:43:4:2:2	-60.6%	80.55	89.52	85.53	88.20	69.82	82.72
		2:8:16:4:2	2:8:43:8:2	-60.6%	80.89	89.40	86.02	87.60	70.06	82.79
		16:16:8	16:43:16	-60.6%	80.03	89.35	85.53	88.60	69.02	82.51

871 B.4 FUSION
872873 The adapter fusion approach of MixLoRA (Li et al., 2024) has been shown to notably improve the
874 performance of additive adapters with LoRA. In Table 9 we report that such approach is helpful for
875 multiplicative adapters such as OperA as well.
876877 Table 9: **Results of the fusion ablation.** We evaluate whether the adapter fusion approach is suc-
878 cessful for OperA/ as well on Llama3-8B and Qwen2.5-3B.
879

Model	Adapter	ARC-c ↑	ARC-e ↑	PIQA ↑	OBQA ↑	BoolQ ↑	Avg ↑
Llama3-8B	OperA (w/o fusion)	73.46	84.30	87.11	86.6	74.07	81.11
	OperA	77.64	86.41	87.6	84.2	74.74	84.19
Qwen2.5-3B	OperA (w/o fusion)	76.54	87.84	82.92	85.8	69.17	80.45
	OperA	80.89	89.40	86.02	87.60	70.06	83.54

891
892
893
894
895
896
897
898
899
900
901
902
903
904
905
906
907
908
909
910
911
912
913
914
915
916
917